

Longwave Radiative Feedback Due to Stratiform and Anvil Clouds

Emily Luschen¹ and James Ruppert¹

¹School of Meteorology, University of Oklahoma, Norman, OK

Key Points:

- A novel column-by-column cloud microphysical classification scheme was developed for application with numerical model output
- Radiative feedback due to stratiform and anvil clouds is a leading driver of tropical convective upscale development
- The local radiative forcing by deep convective regions is similar in magnitude to stratiform but its impact is limited by its smaller area

Corresponding author: Emily Luschen, Emily.W.Luschen-1@ou.edu

Abstract

Studies have implicated the importance of longwave (LW) cloud-radiative forcing (CRF) in facilitating or accelerating the upscale development of tropical moist convection. While different cloud types are known to have distinct CRF, their individual roles in driving upscale development through radiative feedback is largely unexplored. We hypothesize that CRF from stratiform regions will have the greatest effect on upscale tropical convection. We test this hypothesis by analyzing output from convection-permitting ensemble Weather Research and Forecasting (WRF) model simulations of tropical cyclone formation. Using a novel column-by-column cloud classification scheme introduced herein, we use this model output to identify the relative contribution of five cloud types (shallow, congestus, and deep convection; and stratiform and anvil clouds) to the direct LW radiative forcing and the upscale development of convection via LW moist static energy variance. Results indicate that stratiform and anvil regions contribute dominantly to the domain averages of these variables.

Plain Language Summary

Infrared or longwave radiation and its interaction with clouds is important in the formation of tropical storms. Given the different shapes and distributions of distinct cloud types, we hypothesize that they interact with longwave radiation differently, and therefore exert different impacts on the organization of tropical convection. This issue has largely been unexplored. To address this gap, we tested our hypothesis by analyzing numerical model simulations of the formation of two tropical cyclones. Further, we developed a novel cloud classification scheme based on cloud properties that identifies five distinct cloud types. Our results indicate that light-raining regions, such as stratiform and anvil, contribute dominantly to the domain's longwave cloud-radiative heating and the moistening of convective regions. This is due to both these cloud types' strong greenhouse trapping effect and their extensive areal coverage, which spreads this effect over large regions of a developing storm.

1 Introduction

Over the past few decades, we have gained a better understanding of cloud feedbacks and their importance in our climate on a global and regional scale (Zelinka et al., 2020). For example, we now recognize that cloud-radiative forcing (CRF) is an essential maintenance mechanism of the Madden–Julian Oscillation (MJO; Adames & Kim, 2016; Ciesielski et al., 2017; Najarian & Sakaeda, 2023). We have further learned of CRF's part in accelerating tropical cyclone (TC) genesis (e.g., J. H. Ruppert et al., 2020; Wu et al., 2021). However, there remain uncertainties regarding how cloud feedbacks and CRF affect the smaller-scale dynamics of moist convection (Bony et al., 2015).

Studies have begun to highlight the role of CRF in the dynamics of tropical convection (e.g., Bretherton et al., 2005; Wing et al., 2016; J. H. Ruppert et al., 2020), for example, through the study of self-aggregation. Self-aggregation, the spontaneous initiation and clustering of convection, develops in idealized model frameworks that are in radiative-convective equilibrium (RCE), an approximation for the real tropical atmosphere (Manabe & Strickler, 1964; Bretherton et al., 2005). A budget of moist static energy (MSE) variance identifies multiple pathways for promoting convective upscale growth, which shows that it is the longwave (LW) cloud effect that dominates the maintenance of a mature cluster (Muller & Held, 2012; Wing & Cronin, 2016; Wing et al., 2017). The inclusion of rotation provides an idealized analogue for TC development, wherein self-aggregation takes the form of tropical cyclogenesis (Bretherton et al., 2005; Davis, 2015; Wing et al., 2016). Like in non-rotating frameworks, the cloud-LW radiative feedback considerably aids the development of self-aggregation, but differing from non-rotating frameworks, surface flux feedback is also important to aggregation and its maintenance (Wing et al., 2016).

Nonetheless, prior to the development of strong surface winds (i.e., genesis of a surface vortex), the cloud-LW radiative feedback dominates aggregation, which takes the form of upscale convective development (J. H. Ruppert et al., 2020).

Recent studies have applied the concepts from RCE model frameworks into a real-world context and demonstrate that LW CRF indeed accelerates TC development (J. H. Ruppert et al., 2020; Wu et al., 2021). One supported hypothesis for how this works is that LW CRF promotes upward motion in moist regions (Bu et al., 2014; J. H. Ruppert et al., 2020) and, thus, creates a thermally direct circulation that increases moisture in those moist areas (Bretherton et al., 2005; Needham & Randall, 2021a, 2021b). Still, there is limited understanding of how the interaction between clouds, radiative heating, and convective-scale motions manifests in this feedback, which constitutes an important knowledge gap that we seek to address here.

Tropical convection is composed of and closely linked to distinct cloud types, including shallow cumuli, congestus, deep cumulonimbi, stratiform, and anvil clouds (Johnson et al., 1999). These clouds are distinct components of mesoscale convective systems (MCSs), each with unique dynamic behavior, distribution, and composition (Houze Jr., 2004). To our knowledge, no study to date has identified the unique role of specific cloud types on CRF and their resulting influence on convective upscale growth, which is the focus of our study. We specifically address the question of how different cloud types in organized convective systems uniquely promote upscale development through LW radiative forcing.

Given the widespread, blanketing, and long-lived nature of both anvil clouds and stratiform precipitation systems (Webster & Stephens, 1980; Houze, 1997; Schumacher & Houze, 2003; Ahmed & Schumacher, 2015), *we specifically hypothesize that these cloud systems are the most important for promoting convective upscale development through LW CRF.* We examine this hypothesis by determining the contributions of five different cloud types to LW CRF and the LW MSE variance source term using a novel classification scheme that we apply to convection-permitting ensemble Weather Research and Forecasting (WRF) model simulations of tropical organized deep convection. We leverage two TC development events to do so, Super Typhoon Haiyan (2013) and Hurricane Maria (2017), though we emphasize the early simulation periods prior to any intense TCs. While we highlight our analysis of Haiyan, the results from Maria (Supporting Information; SI) support our hypothesis as well. Our results can guide future observational study of CRF. Furthermore, with CRF tied to a primary source of numerical model uncertainty (Morrison et al., 2020; Zelinka et al., 2020), this work may ultimately help identify new pathways to improve the numerical model prediction of weather and climate.

2 WRF Simulations

To quantify the role of different precipitating cloud types on CRF and their associated impact on tropical convection, we simulate the TC development cases for Haiyan and Maria through numerical model simulations. These storms were chosen because they developed in a typical environment for tropical cyclogenesis, including weak vertical wind shear and high sea surface temperatures (SSTs; J. H. Ruppert et al., 2020), and so represent a larger population of TC cases. To support the notion that our results are generalizable, i.e., not specific to post-TC-genesis conditions, we include in SI (Figures S1-S2) our results with only the first 24 hours of the simulation for comparison. The simulations consist of a 10-member ensemble using the Advanced Research Weather Research and Forecasting model (WRF-ARW, version 4.3.1; Skamarock et al., 2021). We use a nested domain with the outer domain's initial and boundary conditions initiated from the first 10 ensemble members of the NOAA-NCEP Global Ensemble Forecast System (2015) retrieved from the NOAA National Centers for Environmental Information. The

model is run with 55 stretched vertical levels with a model top at 10 hPa and a two-nest approach. The inner nest is 3-km grid spacing and approximately $3,600 \times 2,200$ km in scale. The simulations are integrated from 0000 UTC 1–0000 UTC 5 Nov 2013 for Haiyan and 0000 UTC 14–0000 UTC 18 Sept 2017. The microphysics is represented by the two-moment scheme of Thompson and Eidhammer (2014). The simulations have clouds interacting with radiation as in nature using the SW and LW radiation schemes from the Rapid Radiative Transfer Model for GCMs (RRTMG) (Iacono et al., 2008), which is fully coupled to the microphysics scheme. The other physics settings are as in J. H. Ruppert et al. (2020). Our results for Maria are shown in the SI (Figures S3–S4). For all analysis, we exclude the first 12 timesteps as “spin-up” time and 80 points from domain lateral boundaries.

3 Cloud Classification

To investigate our research question, we require a classification algorithm that can accurately identify a range of cloud types. Traditional precipitation classifications rely on low-level reflectivity and its gradients to identify stratiform and convective precipitation (e.g., Steiner et al., 1995; Biggerstaff & Listemaa, 2000; Powell et al., 2016). As we seek to more comprehensively capture three-dimensional cloud coverage, however, we develop a column-by-column scheme that leverages full-column model hydrometeor mass information, similar to Sui et al. (2007). Since it is column-by-column, the scheme can also be effectively implemented during runtime in parallelized model frameworks, which is a strength that we will exploit in a forthcoming study. While the scheme is developed ad hoc for our purposes and is expected to be sensitive to model microphysical scheme choice, its simplicity should make future implementations of the scheme straightforward, subject to adjustments as necessary.

To build confidence in our algorithm, we compare the spatial distributions and mean vertical motion profiles using our classification to that of the traditional reflectivity-based scheme of Rogers (2010), which was developed for application to model output and assigns cloud type based on reflectivity at 0.4 and 3 km elevation. Although we make this comparison to a reflectivity-based classification, we neither expect nor desire our results to perfectly match, since the motivation behind each algorithm is different. A scheme based on low-level reflectivity will likely underestimate or incorrectly classify stratiform and anvil regions considering reflectivity’s sensitivity to large rain drops and high rain rates. Since cloud–radiation interaction is not limited to strongly precipitating clouds, we have designed our algorithm with the goal of capturing this broader population of radiatively interactive clouds.

Most classification schemes are limited to three precipitation categories: convective, stratiform, and a third category dependent on the algorithm. The scheme by Rogers (2010) includes anvil as its third category and the Sui et al. (2007) classification contains a mixed category between convective and stratiform. We use the model hydrometeor information in our scheme to further separate the categories, which include deep convective, shallow convective, congestus, stratiform, anvil, and non-precipitating. In summary, we seek to develop an approach that leverages model microphysical information, captures the bulk convective and stratiform behavior as validated using well-established paradigms of vertical motion, and includes additional classification sub-types to capture their distinct radiative forcing signatures.

3.1 Description and Development

Our classification is summarized in Figure 1. The first step of our classification determines if a cell contains cloud. This decision is determined via a total water path (TWP; the sum of rain, cloud, graupel, snow, and ice column-integrated mixing ratios) threshold of 0.1 mm. We found a TWP threshold to be a necessary cutoff to exclude many grid columns identified as containing spurious (i.e., small magnitude) hydrometeor amounts

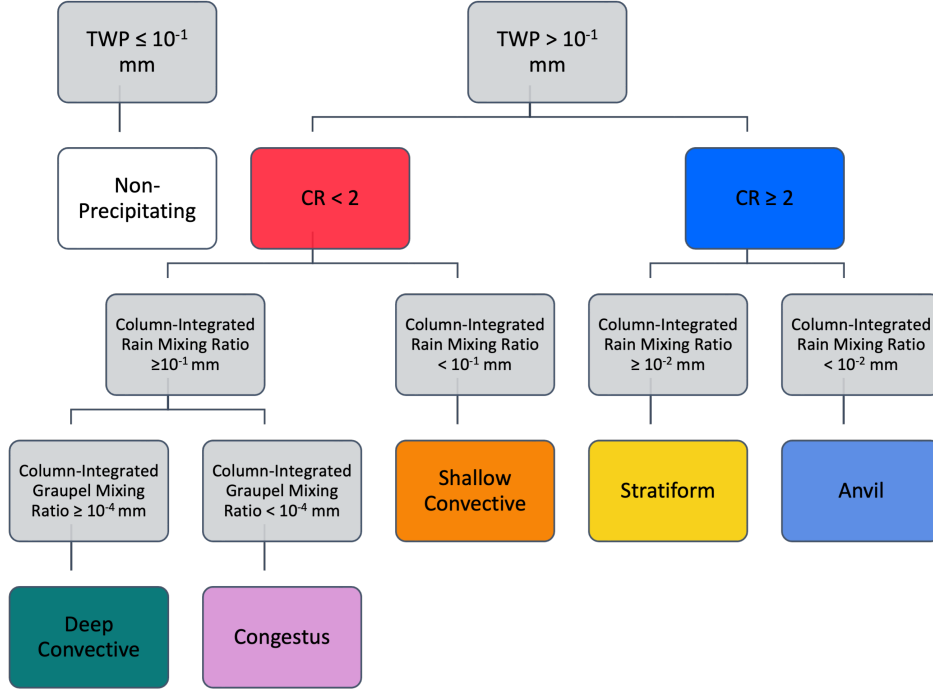


Figure 1. Flow chart summarizing the categorization process for our precipitation classification algorithm.

associated with negligible rainfall and radiative forcing. We compared this TWP threshold to Rogers (2010) to confirm we were not cutting out a large population of cloud (Figure S5). Adjustments to the TWP threshold primarily effects shallow convective and anvil domain fractions, but does not strongly alter the radiative forcing statistics (not shown).

Next, bulk convective and stratiform categories are separated by a cloud ratio (CR) threshold, as in Sui et al. (2007). The CR is the ratio of ice water path (IWP) to liquid water path (LWP). IWP is the sum of column-integrated graupel, snow, and cloud ice mixing ratios and LWP is the sum of column-integrated rain and cloud water mixing ratios. Columns with a $CR < 2$ are considered convective and columns with $CR \geq 2$ are considered stratiform, assuming stratiform regions will be dominated by ice hydrometeors. We again compared the CR threshold to the Rogers (2010) scheme and confirmed our threshold falls between its identified convective and stratiform populations (Figure S6). Convective regions are further divided between deep convective, congestus, and shallow, as follows. Grid cells are marked shallow if the column-integrated rain mixing ratio falls below a threshold of 0.1 mm considering that congestus and deep convective regions would have higher rain rates (Johnson et al., 1996). Deep convective is separated from congestus by a graupel mixing ratio threshold of 10^{-4} mm, with deep convective regions exceeding this threshold, on the basis that congestus have limited vertical extent beyond the 0°C level (Johnson et al., 1999) and hence limited glaciation. Stratiform is separated from anvil where columns exceed a rain mixing ratio of 0.01 mm, accounting for stratiform having more precipitating liquid water content than anvil clouds (Houze, 1997; Houze Jr., 2004). While we lack a means for comparing these sub-classifications with the traditional algorithm, we assess their averaged vertical motion profiles against well-established vertical structures in convective and stratiform precipitation (Steiner et al., 1995; Houze Jr., 2004) in the following subsection.

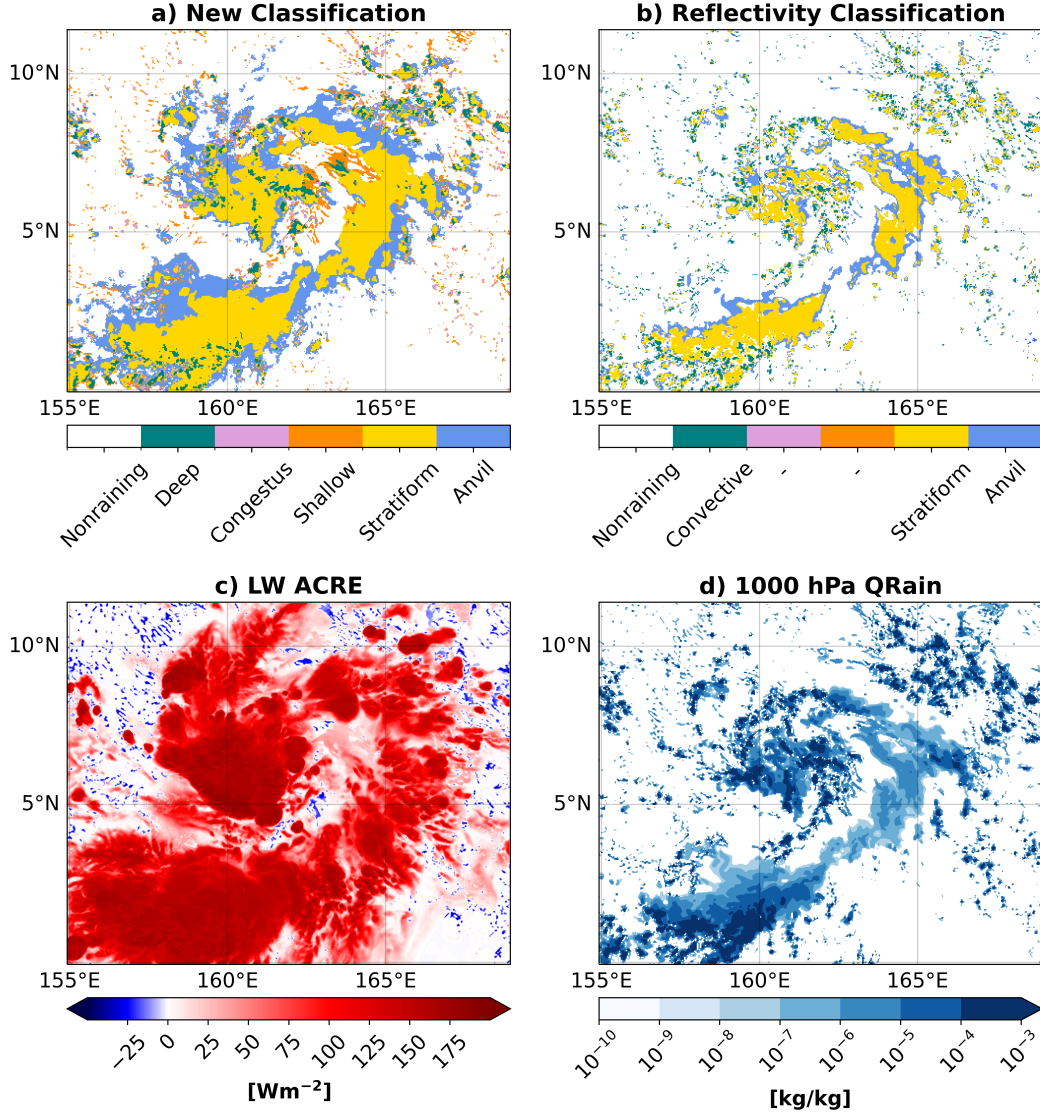


Figure 2. Maps comparing a) the new classification scheme, the b) traditional reflectivity classification, c) the LW ACRE, and d) 1000 hPa rain water mixing ratio. See color bars for algorithm classifications. All panels show the first ensemble member of Haiyan at 36 hours.

3.2 Comparison and Validation

We first present horizontal maps (Figure 2) comparing the new algorithm and the Rogers (2010) classification. The new classification produces the following cloud fractions for the domain shown (Figure 2): deep convective as 2.76%, congestus as 1.39%, shallow convective as 4.04%, stratiform as 16.42%, anvil as 13.99%, and non-precipitating as 61.4%. The reflectivity approach produces the following cloud fractions: convective is 3.53%, stratiform is 10.09%, anvil is 6.98%, and non-precipitating is 79.4%. The new classification marks more grid cells within the domain as cloud while also increasing the number of points identified as anvil and stratiform compared to the reflectivity approach. The increased count for these cloud types indicates that our algorithm is more sensitive to cloudy columns with lower rain rates, which is an expected and intended result, given our objectives. Additionally, we see more stratiform and anvil regions enveloping the deep

convection regions, the latter of which are often located on edges with the reflectivity-based algorithm. Our algorithm also identifies shallow convection, which is incorporated with the general convective category when using reflectivity.

We next present the vertical motion (w) profiles averaged for each cloud type in our classification alongside the adapted Rogers (2010) scheme in Figure 3a-c. All three convective w -profiles have an expected bottom-heavy profile, with deep convective maximizing around 550 hPa, congestus maximizing at 850 hPa, and shallow convective maximizing at 900 hPa. The profile averaged across all three convective types is consistent with the shape of reflectivity-based classification profile, albeit with a smaller magnitude and broader peak. These differences are consistent with the capture of more weakly precipitating columns of convection in the new algorithm. Further, for both stratiform and anvil the new algorithm produces a “top-heavy” profile, with upper-level rising and low-level sinking motion, with anvil having a smaller magnitude than stratiform. In comparison with the reflectivity-based approach, the profiles are similar in shape but with slight differences in magnitudes and with our classification having a 50-100 hPa higher inflection point. The overall merit of this new classification scheme is supported by the consistencies between these w -profiles in the two algorithms and, more broadly, with well-established paradigms documented in the literature (Steiner et al., 1995; Houze, 1997; Houze Jr., 2004).

We conclude that the new classification algorithm accurately identifies precipitation types for this model output. The scheme is less computationally bulky than traditional reflectivity-based schemes as it is based on microphysics thresholds and is a column-by-column approach. This allows for cloud classification within the framework of models without the need of neighboring cell information, which is computationally cumbersome in highly parallelized frameworks commonly used for convective-scale modeling. However, this approach does have some weaknesses. By having the cloud classification based on microphysics thresholds, the scheme inherently relies on specific hydrometeor behavior and treatment. Different microphysics schemes have vastly different treatments of hydrometeors (Morrison et al., 2020) and would hence require modification to apply to other microphysics schemes. This caveat extends to reflectivity-based approaches, however, since model-based reflectivity relies upon microphysical assumptions. Additionally, the new algorithm can only identify one cloud type per column. So, if there are layers of different cloud types present, only the most prominent type will be identified. Despite these limitations, we deem our algorithm suitable for our science question.

4 Longwave Radiative Features of Different Cloud Types

4.1 ACRE and CRF

We next seek to quantify each cloud mode’s contribution to LW CRF and ACRE. Using our column-by-column based classification algorithm, we calculate the domain-averaged and class-averaged LW ACRE. The *domain* average measures each cloud types’ contribution to the total LW ACRE in the domain, while the *class* average calculates the mean LW ACRE averaged only over the cells of that type. Stratiform and anvil modes contribute the most to the domain-averaged LW ACRE, with averages around 10 W m^{-2} (Figure 4a). Of the convective types, deep convective has the greatest contribution to the LW ACRE (2.5 W m^{-2}), with congestus and shallow convective points providing the smallest contributions. The large contribution to the domain average by stratiform and anvil modes is partly due to the larger area coverage of these cloud types (Figure 2a,b).

But area coverage is not the only reason stratiform and anvil regions have the greatest domain-averaged LW ACRE. When averaging ACRE by class, stratiform and anvil regions retain the highest ACRE value (Figure 4b). They are almost an order of mag-

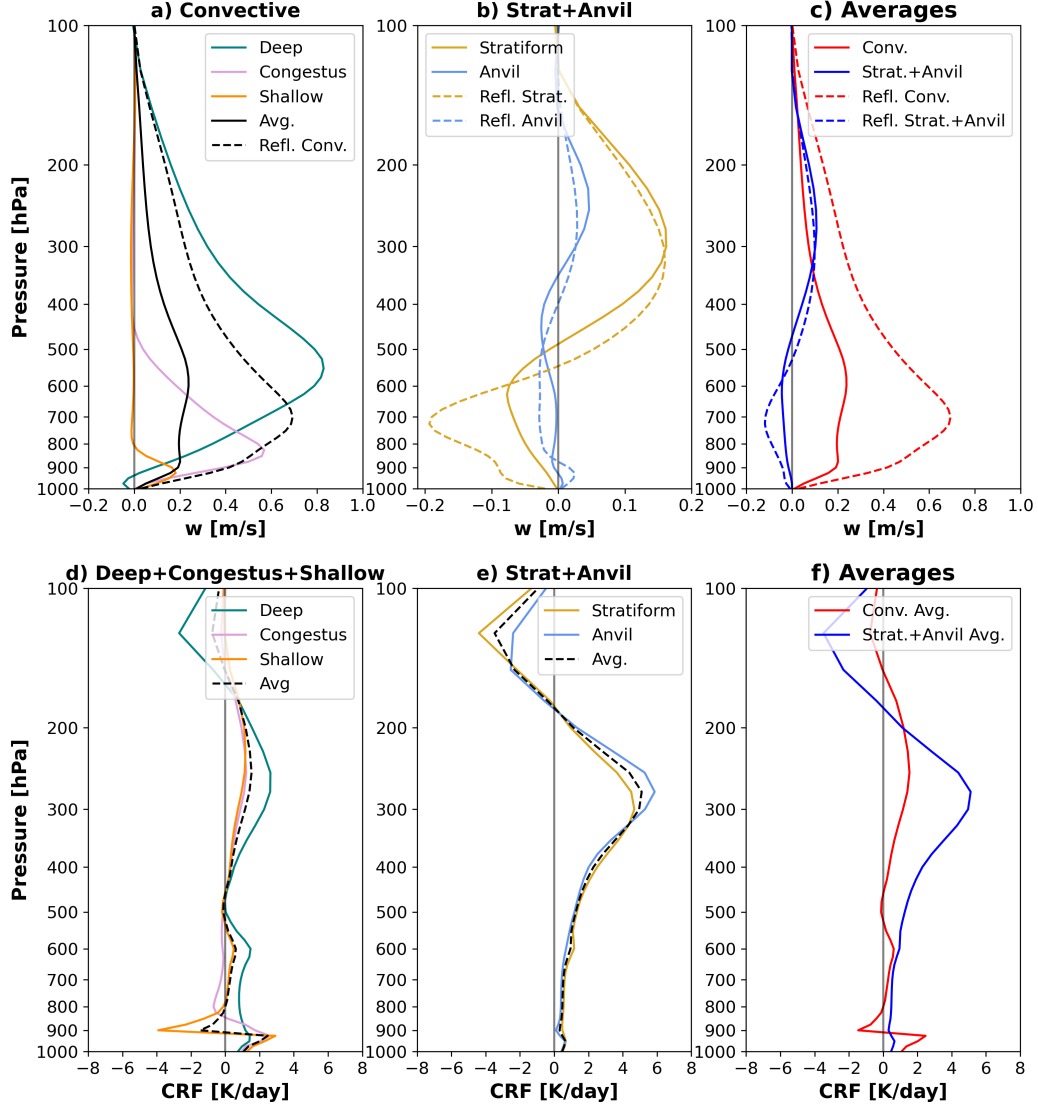


Figure 3. Averaged profiles of vertical motion (w) (a-c) and CRF (d-f) in convective categories (left column), stratiform and anvil (middle column), and the total convective and stratiform categories (right column). In (a-c), the new classification is presented in solid lines and the reflectivity approach appear as dashed. In (d,e), the dashed black lines represent the averages across all shown categories within the respective panel. Plots include values from all 10 members and 85 timesteps of Haiyan.

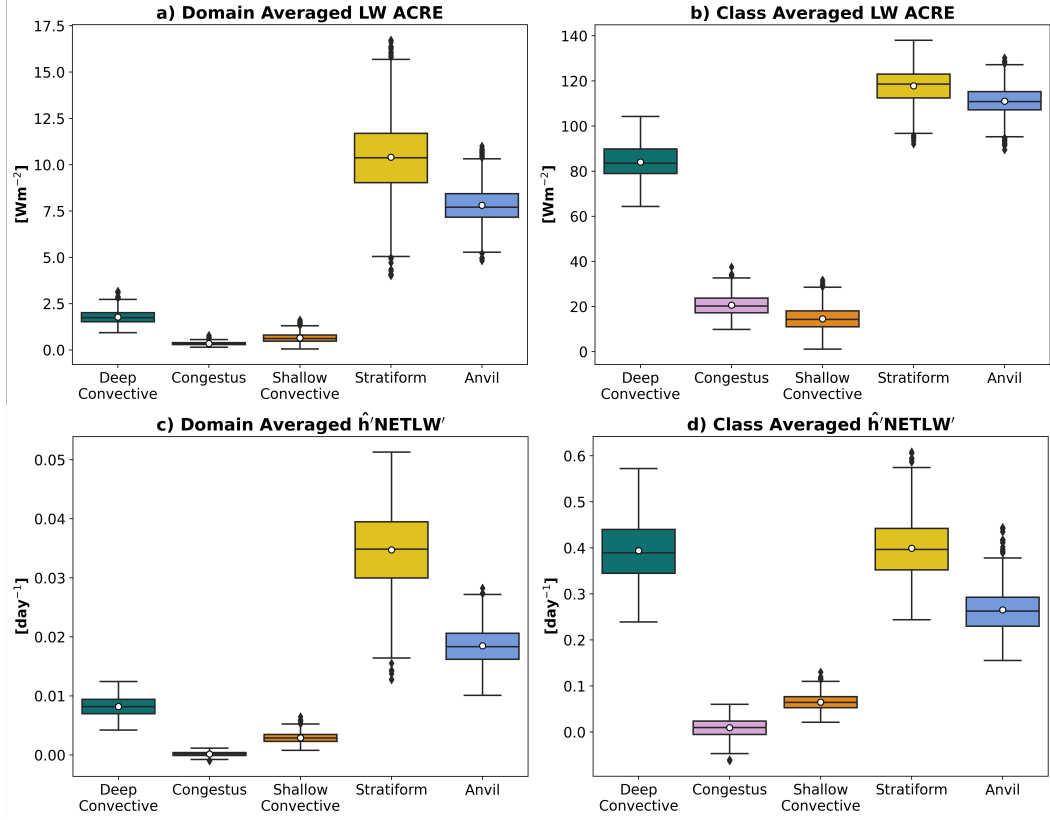


Figure 4. Boxplots of domain-averaged (left) and class-averaged (right) LW ACRE (top) and $\hat{h}'NETLW'$ (bottom) by precipitation type. White circles indicate the mean value. Black diamonds represent outliers. Domain averages represent class-averaged values normalized by total grid cell count, and class-averaged values are normalized only by category cell count. Plots include values from all 10 members and 85 timesteps of Haiyan.

nititude greater than that of the congestus and shallow convective types. Deep convective has the greatest LW ACRE value of the three convective modes, with an average value of 85 W m^{-2} . This value is comparable in magnitude to that of stratiform and anvil regions, suggesting comparable radiative forcing by these categories within a given column. The combination of stratiform and anvil's large class-averaged LW ACRE with their larger area coverage explains their much larger contribution to the domain-averaged LW ACRE.

We next present vertical profiles of LW CRF to aid interpretation of these results (Figure 3d-f). Cloud types with larger ACRE values exhibit a deep layer of positive CRF. Stratiform and anvil modes are similar in CRF shape and magnitude, which is noteworthy given their much different vertical motion magnitude (Figure 3b). Namely, the radiative forcing per unit vertical mass flux within a given layer is much larger for anvil than stratiform. CRF in these cloud modes is positive from 200 hPa to the surface and with maxima around 5 K day^{-1} at 300 hPa, with strong cloud-top cooling above 200 hPa. Of the convective categories, deep convective has the deepest layer of positive CRF of 2 K day^{-1} from 200 hPa to the surface, with a small layer near 0 K day^{-1} between 400 and 500 hPa. This may be due to layers of detrained cloud in association with the 0°C stable layer (Johnson et al., 1996). Like stratiform and anvil, deep convective has a strong signature of cloud-top cooling above 200 hPa. Congestus and shallow convective modes have maxima in the lower troposphere with cooling above due to their low cloud-top height. Above 800 hPa, their CRF hovers around 0 K day^{-1} . The modest heating values in the upper troposphere in these categories are likely a result of the algorithm only identifying one cloud type for each column, with these columns potentially including thin anvil clouds. Otherwise, these results are consistent with expectations of cloud depth based on mean vertical motion (Figure 3 a-c).

4.2 LW MSE Variance Source Term

The MSE budget is a tool that allows us to assess and quantify upscale development and intensification of convection. This tool has been used to assess the influence of radiative feedback in relation to both self-aggregation (Wing & Emanuel, 2014) and TC genesis (J. H. Ruppert et al., 2020; Wu et al., 2021). Our interest in this budget is primarily in the LW-source term as it has been shown to be the dominant term for maintaining and accelerating convective upscale development (at least, prior to TC genesis) (Wing & Emanuel, 2014; Wing & Cronin, 2016; J. H. Ruppert et al., 2020). The LW MSE variance term ($\hat{h}'\text{NetLW}'$) is the correlation between the anomaly of the density-weighted vertical integral of MSE (\hat{h}') and the anomalous column LW radiative flux convergence (NetLW'), where anomalies are calculated as the deviation from the domain average. More details on the calculation of this term can be found in Wing and Emanuel (2014) and J. H. Ruppert et al. (2020).

When we average $\hat{h}'\text{NetLW}'$ by cloud type, we once again see that stratiform and anvil regions contribute the most to the domain-averaged LW MSE variance source term. Stratiform dominates, with an average of about 0.035 day^{-1} (Figure 4c). The stratiform regions also have the highest class-averaged LW MSE variance of all the cloud types (Figure 4d). Congestus and shallow convective points have the lowest class-averaged LW MSE variance, as may be anticipated from LW ACRE (Figure 4 a-b). Surprisingly, deep convective regions have the second highest LW MSE variance, almost matching that of stratiform. Anvil's class average follows deep convective with a value of 0.25 day^{-1} compared to stratiform and deep convective's averages of about 0.4 day^{-1} . Like the LW ACRE, the stratiform and anvil regions have much greater areal coverage than convective regions (Figure 2a), which explains the smaller domain-averaged value for convection.

The high column influence of stratiform and anvil clouds in terms of both LW ACRE and $\hat{h}'\text{NetLW}'$, combined with their extensive areal coverage, indicates their unique im-

portance for supporting upscale convective development in the tropics by amplifying MSE variance via radiative forcing. Although deep convective regions also have high values of LW MSE variance in a given column, the small regional coverage of this cloud type likely limits its area-averaged impact, which is how radiative forcing is linked to the tendency of MSE variance (Wing & Emanuel, 2014). These findings emphasize the important influences of stratiform and anvil regions on tropical convective organization through their radiative forcing, which have not been previously examined in this manner.

5 Summary and Conclusions

In this study, we have investigated the role of CRF of five different cloud types and their ability to aid the organization of tropical convection via the analysis of convection-permitting WRF simulations conducted in the context of TC development. To accomplish this, we developed a novel column-by-column cloud classification algorithm based on microphysical thresholds. Our classification holds several advantages over low-level reflectivity-based approaches, such as it is computationally efficient and can be run within the framework of a numerical model, it is sensitive to cloud (including non-precipitating) throughout the column, and it identifies five cloud modes (instead of two or three): shallow, congestus, and deep convective; and stratiform and anvil. However, the disadvantages to this algorithm includes its likely sensitivity to different microphysics schemes based on its threshold approach and that it can only identify one cloud type per column. Despite these disadvantages, this approach to cloud classification allows for more questions to be answered on the influence of cloud type, including our question of how different cloud types in organized convective systems promote upscale development through LW radiative forcing.

We hypothesized that stratiform and anvil regions would support convective organization more than other categories through LW ACRE and the LW MSE variance source term. We found that stratiform and anvil contributed the most to the domain-averaged ACRE and had greater class-averaged ACRE than that of the other types, indicating their important contribution to the direct LW radiative forcing. For the LW MSE variance source term, stratiform and anvil again contributed the most to the domain average. However, the class averages revealed that deep convective was on par with stratiform regions, resulting in those two classes having the highest class averages. Anvil was third highest, followed by shallow and congestus, which were much weaker. While the class-averaged LW MSE variance source term indicates that the localized forcing by deep convective, stratiform, and anvil clouds is comparable, anvil and stratiform clouds dominate in supporting convective upscale development owing to their much greater area coverage. Although we do not fully answer the question of how different cloud types in organized convective systems uniquely promote upscale development through LW radiative forcing, we do provide support of our hypothesis and shed new light on the specific cloud types most important to convective upscale via LW cloud feedback. Future work will focus on the mechanisms CRF works through to promote organization within tropical convection.

Open Research Section

The code needed to recreate the WRF simulations described in this study is published at Zenodo (J. Ruppert & Zhang, 2024). The code for the precipitation classification algorithm (Luschen & Ruppert, 2024b) and the analysis (Luschen & Ruppert, 2024a) presented here are available on Zenodo as well.

Acknowledgments

We acknowledge Rosimar Rios-Berrios, Yunji Zhang, Shun-Nan Wu, Naoko Sakaeda, and Greg McFarquar for their feedback on this work. This project was supported by the National Science Foundation under projects 1712290 and 2331120. This material is based upon work supported by the National Science Foundation Graduate Research Fellowship under Grant No. (NSF grant number). We also acknowledge the Texas Advanced Computing Center (TACC; <http://www.tacc.utexas.edu>) at The University of Texas at Austin for high-performance computing resources (the Stampede2 machine) that have contributed to this research.

References

- Adames, Á. F., & Kim, D. (2016, mar). The MJO as a Dispersive, Convectively Coupled Moisture Wave: Theory and Observations. *Journal of the Atmospheric Sciences*, 73(3), 913–941. doi: 10.1175/JAS-D-15-0170.1
- Ahmed, F., & Schumacher, C. (2015). Convective and stratiform components of the precipitation-moisture relationship. *Geophysical Research Letters*, 42(23), 10,453–10,462. doi: 10.1002/2015GL066957
- Biggerstaff, M. I., & Listemaa, S. A. (2000, December). An Improved Scheme for Convective/Stratiform Echo Classification Using Radar Reflectivity. *Journal of Applied Meteorology and Climatology*, 39(12), 2129–2150. doi: 10.1175/1520-0450(2001)040<2129:AISFCS>2.0.CO;2
- Bony, S., Stevens, B., Frierson, D. M. W., Jakob, C., Kageyama, M., Pincus, R., . . . Webb, M. J. (2015, April). Clouds, circulation and climate sensitivity. *Nature Geoscience*, 8(4), 261–268. doi: 10.1038/ngeo2398
- Bretherton, C. S., Blossey, P. N., & Khairoutdinov, M. (2005, December). An Energy-Balance Analysis of Deep Convective Self-Aggregation above Uniform SST. *Journal of the Atmospheric Sciences*, 62(12), 4273–4292. doi: 10.1175/JAS3614.1
- Bu, Y. P., Fovell, R. G., & Corbosiero, K. L. (2014, May). Influence of Cloud–Radiative Forcing on Tropical Cyclone Structure. *Journal of the Atmospheric Sciences*, 71(5), 1644–1662. doi: 10.1175/JAS-D-13-0265.1
- Ciesielski, P. E., Johnson, R. H., Jiang, X., Zhang, Y., & Xie, S. (2017). Relationships between radiation, clouds, and convection during DYNAMO. *Journal of Geophysical Research: Atmospheres*, 122(5), 2529–2548. doi: 10.1002/2016JD025965
- Davis, C. A. (2015, September). The Formation of Moist Vortices and Tropical Cyclones in Idealized Simulations. *Journal of the Atmospheric Sciences*, 72(9), 3499–3516. doi: 10.1175/JAS-D-15-0027.1
- Houze, R. A. (1997, oct). Stratiform Precipitation in Regions of Convection: A Meteorological Paradox? *Bulletin of the American Meteorological Society*, 78(10), 2179–2196. doi: 10.1175/1520-0477(1997)078<2179:SPIROC>2.0.CO;2
- Houze Jr., R. A. (2004). Mesoscale convective systems. *Reviews of Geophysics*, 42(4). doi: 10.1029/2004RG000150
- Iacono, M. J., Delamere, J. S., Mlawer, E. J., Shephard, M. W., Clough, S. A., & Collins, W. D. (2008). Radiative forcing by long-lived greenhouse gases: Calculations with the AER radiative transfer models. *Journal of Geophysical Research: Atmospheres*, 113(D13). doi: 10.1029/2008JD009944
- Johnson, R. H., Ciesielski, P. E., & Hart, K. A. (1996, jul). Tropical Inversions near the 0°C Level. *Journal of the Atmospheric Sciences*, 53(13), 1838–1855. doi: 10.1175/1520-0469(1996)053<1838:TINTL>2.0.CO;2
- Johnson, R. H., Rickenbach, T. M., Rutledge, S. A., Ciesielski, P. E., & Schubert, W. H. (1999, aug). Trimodal Characteristics of Tropical Convection. *Journal of Climate*, 12(8), 2397–2418. doi: 10.1175/1520-0442(1999)012<2397:TCOTC>2.0.CO;2

- Luschen, E., & Ruppert, J. (2024a, 2). *Analysis Code for Geophysical Research Letter paper*. doi: 10.5281/zenodo.10645132
- Luschen, E., & Ruppert, J. (2024b, 2). *Column-based Precipitation Classification Algorithm*. doi: 10.5281/zenodo.10611873
- Manabe, S., & Strickler, R. F. (1964, July). Thermal Equilibrium of the Atmosphere with a Convective Adjustment. *Journal of the Atmospheric Sciences*, 21(4), 361–385. doi: 10.1175/1520-0469(1964)021<0361:TEOTAW>2.0.CO;2
- Morrison, H., van Lier-Walqui, M., Fridlind, A. M., Grabowski, W. W., Harrington, J. Y., Hoose, C., ... Xue, L. (2020). Confronting the Challenge of Modeling Cloud and Precipitation Microphysics. *Journal of Advances in Modeling Earth Systems*, 12(8), e2019MS001689. doi: 10.1029/2019MS001689
- Muller, C. J., & Held, I. M. (2012, August). Detailed Investigation of the Self-Aggregation of Convection in Cloud-Resolving Simulations. *Journal of the Atmospheric Sciences*, 69(8), 2551–2565. doi: 10.1175/JAS-D-11-0257.1
- Najarian, H., & Sakaeda, N. (2023). The Influence of Cloud Types on Cloud-Radiative Forcing During DYNAMO/AMIE. *Journal of Geophysical Research: Atmospheres*, 128(8), e2022JD038006. doi: 10.1029/2022JD038006
- Needham, M. R., & Randall, D. A. (2021a). Linking Atmospheric Cloud Radiative Effects and Tropical Precipitation. *Geophysical Research Letters*, 48(14), e2021GL094004. doi: 10.1029/2021GL094004
- Needham, M. R., & Randall, D. A. (2021b). Riehl and Malkus Revisited: The Role of Cloud Radiative Effects. *Journal of Geophysical Research: Atmospheres*, 126(16), e2021JD035019. doi: 10.1029/2021JD035019
- NOAA-NCEP Global Ensemble Forecast System. (2015). *NCEP GFS 0.25 Degree Global Forecast Grids Historical Archive*. UCAR/NCAR - Research Data Archive. doi: 10.5065/D65D8PWK
- Powell, S. W., Houze, R. A., & Brodzik, S. R. (2016, March). Rainfall-Type Categorization of Radar Echoes Using Polar Coordinate Reflectivity Data. *Journal of Atmospheric and Oceanic Technology*, 33(3), 523–538. doi: 10.1175/JTECH-D-15-0135.1
- Rogers, R. (2010, January). Convective-Scale Structure and Evolution during a High-Resolution Simulation of Tropical Cyclone Rapid Intensification. *Journal of the Atmospheric Sciences*, 67(1), 44–70. doi: 10.1175/2009JAS3122.1
- Ruppert, J., & Zhang, Y. (2024, 2). *Ensemble WRF Simulations of Typhoon Haiyan and Hurricane Maria*. doi: 10.5281/zenodo.10572959
- Ruppert, J. H., Wing, A. A., Tang, X., & Duran, E. L. (2020, November). The critical role of cloud–infrared radiation feedback in tropical cyclone development. *Proceedings of the National Academy of Sciences*, 117(45), 27884–27892. doi: 10.1073/pnas.2013584117
- Schumacher, C., & Houze, R. A. (2003, jun). Stratiform Rain in the Tropics as Seen by the TRMM Precipitation Radar*. *Journal of Climate*, 16(11), 1739–1756. Retrieved from [http://journals.ametsoc.org/doi/10.1175/1520-0442\(2003\)016%3C1739:SRITTA%3E2.0.CO;2](http://journals.ametsoc.org/doi/10.1175/1520-0442(2003)016%3C1739:SRITTA%3E2.0.CO;2) doi: 10.1175/1520-0442(2003)016<1739:SRITTA>2.0.CO;2
- Skamarock, W. C., Klemp, J. B., Dudhia, J. B., Gill, D. O., Barker, D. M., Duda, M. G., ... Powers, J. G. (2021). A Description of the Advanced Research WRF Model Version 4.3. *NCAR Technical Note*(July), 1–165. doi: 10.5065/1dfh-6p97
- Steiner, M., Houze, R. A., & Yuter, S. E. (1995, September). Climatological Characterization of Three-Dimensional Storm Structure from Operational Radar and Rain Gauge Data. *Journal of Applied Meteorology and Climatology*, 34(9), 1978–2007. doi: 10.1175/1520-0450(1995)034<1978:CCOTDS>2.0.CO;2
- Sui, C.-H., Tsay, C.-T., & Li, X. (2007). Convective–stratiform rainfall separation by cloud content. *Journal of Geophysical Research: Atmospheres*, 112(D14). doi: 10.1029/2006JD008082

- Thompson, G., & Eidhammer, T. (2014, October). A Study of Aerosol Impacts on Clouds and Precipitation Development in a Large Winter Cyclone. *Journal of the Atmospheric Sciences*, 71(10), 3636–3658. doi: 10.1175/JAS-D-13-0305.1
- Webster, P. J., & Stephens, G. L. (1980, jul). Tropical Upper-Tropospheric Extended Clouds: Inferences from Winter MONEX. *Journal of the Atmospheric Sciences*, 37(7), 1521–1541. Retrieved from <http://journals.ametsoc.org/doi/abs/10.1175/1520-0469-37.7.1521> doi: 10.1175/1520-0469-37.7.1521
- Wing, A. A., Camargo, S. J., & Sobel, A. H. (2016, July). Role of Radiative–Convective Feedbacks in Spontaneous Tropical Cyclogenesis in Idealized Numerical Simulations. *Journal of the Atmospheric Sciences*, 73(7), 2633–2642. doi: 10.1175/JAS-D-15-0380.1
- Wing, A. A., & Cronin, T. W. (2016). Self-aggregation of convection in long channel geometry. *Quarterly Journal of the Royal Meteorological Society*, 142(694), 1–15. doi: 10.1002/qj.2628
- Wing, A. A., Emanuel, K., Holloway, C. E., & Muller, C. (2017). Convective Self-Aggregation in Numerical Simulations: A Review. *Surveys in Geophysics*, 38(6). doi: 10.1007/s10712-017-9408-4
- Wing, A. A., & Emanuel, K. A. (2014). Physical mechanisms controlling self-aggregation of convection in idealized numerical modeling simulations. *Journal of Advances in Modeling Earth Systems*, 6(1), 59–74. doi: 10.1002/2013MS000269
- Wu, S.-N., Soden, B. J., & Nolan, D. S. (2021). Examining the Role of Cloud Radiative Interactions in Tropical Cyclone Development Using Satellite Measurements and WRF Simulations. *Geophysical Research Letters*, 48(15), e2021GL093259. doi: 10.1029/2021GL093259
- Zelinka, M. D., Myers, T. A., McCoy, D. T., Po-Chedley, S., Caldwell, P. M., Ceppi, P., . . . Taylor, K. E. (2020). Causes of higher climate sensitivity in cmip6 models. *Geophysical Research Letters*, 47(1), e2019GL085782. doi: <https://doi.org/10.1029/2019GL085782>